S & M 4000

Evolution Characteristics of Future Climate Change in Northeast China

Zheng Chu,[1,2,3] Lingyan Wang,[1*] Yanghui Ji,[2,3**] Baocai Zhou,[2,3]
Jingjin Gong,[2,3] Qiujing Wang,[2,3] and Li Chen[4]

[1]Harbin Normal University, 1st Shida RD, Songbei District, Harbin City, Heilongjiang Province 150025, China
[2]Heilongjiang Meteorological Science Research Institute,
71 Diantan Rd, Xiangfang District, Harbin City, Heilongjiang Province 150030, China
[3]Wuying National Climatological Observatory,
Wuying town, Fenglin County, Yichun City, Heilongjiang Province 153000, China
[4]Heilongjiang Climate Center,
71 Diantan Rd, Xiangfang District, Harbin City, Heilongjiang Province 150030, China

(Received October 1, 2024; accepted April 4, 2025)

Keywords: climate change, spatiotemporal characteristics, Northeast China

On the basis of the meteorological data in the low-emission representative concentration pathway (RCP) 4.5 and high-emission RCP8.5 scenarios from the regional climate model output for 2021–2099, spatiotemporal changes in mean annual temperature, annual precipitation, and the average daily radiation in Northeast China in the future were analyzed using statistical methods in this study. The results are as follows. (1) The mean annual temperatures in the RCP4.5 and RCP8.5 scenarios are 6.26 and 7.36 °C, respectively, both showing a trend of significant increase. The increase rate in the RCP8.5 scenario is higher; there are more years with abrupt change in the RCP4.5 scenario. The temperature in the RCP4.5 scenario has two periods of 2 and 4 years, whereas that in the RCP8.5 scenario is composed of two periods that fail the significance test. The empirical orthogonal functions (EOFs) of the first feature vector fields in the RCP4.5 and RCP8.5 scenarios are 90.26 and 96.61%, respectively. The change types are consistent, and the sensitive areas of variation mainly appear in the western and northern regions. (2) The annual precipitation in the RCP4.5 and RCP8.5 scenarios are 959.95 and 949.02 mm, respectively, showing a nonsignificant increase trend. Among them, abrupt changes in annual precipitation are more frequent in the RCP8.5 scenario, and there are 2 and 6 years in the RCP4.5 scenario and 3 and 5 years in the RCP8.5 scenario. The EOFs of the first three feature vectors are 65.66 and 66.77%. (3) The average daily radiation are 8.56 and 8.80 MJ/(m^2·d) in the RCP4.5 and RCP8.5 scenarios, respectively, both showing a significant increase trend, with a higher increase rate in the RCP8.5 scenario. The abrupt changes in the two scenarios show a large difference, and radiation in the RCP4.5 scenario has a 4-year period and that in the RCP8.5 scenario has a 3-year period. The EOFs of the first three feature vectors are 66.47 and 81.38% in the RCP4.5 and RCP8.5 scenarios, respectively.

[*]Corresponding author: e-mail: wangly137@126.com
[**]Corresponding author: e-mail: jyh7977@126.com
https://doi.org/10.18494/SAM5386

1. Introduction

In August 2021, the sixth assessment report of the Intergovernmental Panel on Climate Change (IPCC) pointed out that the anthropogenic change in global average surface temperature from 2010 to 2019 was 0.8–1.3 °C compared with that from 1850 to 1900.(1) To date, studies have shown that in the next 50 to 80 years, the global average temperature will continue to increase. Global warming will lead to more serious atmospheric evaporation and drought events in the world, with the global temperature increase stabilizing at 1.5 to 2.0 °C (Trustworthy Computing). Some areas will experience more frequent and severe agricultural and ecological disasters. When the global temperature increase reaches 4 °C, the ecosystems of about 50% of human settlements will be affected.(2,3) Therefore, understanding the law of climate change and mastering the mechanism are important for people to seek advantages in the future, avoid disadvantages, and adapt to climate change.(4) The most direct expression of climate change are the changes in meteorological elements such as radiation, temperature, and precipitation. Therefore, it is valuable to analyze the law of changes in meteorological elements, the effects of climate change, and the ways of solving climate change problems in future scientific research.

Advances in sensor technology have expanded the capabilities of real-time monitoring and climate change detection. Multisource data fusion techniques are increasingly employed to integrate data from different sensors, improving the robustness of climate projections. In particular, the fusion of remote sensing data with ground station observations enhances the accuracy of regional climate models (RCMs), such as those employed in CMIP5 representative concentration pathway (RCP) scenarios. This integration not only addresses the limitations of individual sensor systems but also reduces uncertainties in predicting future climate changes.

In the study of changes in meteorological elements, the research methods used vary greatly depending on research time. The analysis of climate change in historical time series is mainly based on observational meteorological data. Ancient books and documents were usually used for mining data from hundreds of years ago;(5,6) items of evidence such as tree rings, ice cores, and corals are needed to obtain the final conclusion on climate a thousand years ago or in paleoclimate research.(7,8) In the study of future climate change, for which there is no meteorological data, climate model simulation is often used for research. From the spatial scale, climate models can be divided into the global circulation model (GCM) and the regional climate model (RegCM). There is still uncertainty in the simulation results for each model because of differences in time and space. Compared with GCM, RegCM performs better in simulating specific regions.(9) When predicting future climate change, emission scenarios combined with RegCM are adopted, such as the AB series by IPCC AR4 and the RCP series by IPCC AR5. The output of multiple meteorological elements (such as temperature and precipitation) is discussed and coupled with those of other models (e.g., agricultural and hydrological models) for more in-depth research to draw a conclusion about the impact of future climate change on all aspects.(10–12)

Northeast China, at the highest latitude in China, is a strategic production base for food security and one of the regions most affected by global climate change. At 45° north latitude, Northeast China, which includes Heilongjiang, Jilin, and Liaoning provinces and Dongsimeng of Inner Mongolia, is a semi-arid region climate zone called the Golden Corn Belt of the World.[13] Research on climate change in Northeast China was carried out earlier, initially using the historical observation data for Northeast China to analyze the spatiotemporal variation characteristics of climate elements such as temperature, precipitation, and wind speed.[14] A separate analysis of different times and spaces was also carried out.[15] There have also been many studies on analyzing the impacts of climate change on, for example, ecology, water temperature, human activities, and agriculture and responses,[16] among which, agriculture was found to be affected most profoundly. In terms of the impacts of agroclimatic resources, extreme weather, and disasters on agriculture, different scholars used different research targets such as corn, rice, soybeans, and other food crops to study the adaptation and response of Northeast China to climate change. Such studies deepen our understanding of climate change in Northeast China and will ultimately enable the achivement of the advantages and avoidance of the disadvantages.

Over the past 50 years, the temperature increase rate in Northeast China has been about 0.36 °C/10a within the background of climate warming; this value is higher than the national temperature increase rate. This temperature increase also affects the ecological environment and will aggravate the frequency of severe weather in the future and make Northeast China one of the regions with the largest fluctuations in grain yield in China.[17] The impact of climate change on Northeast China has great uncertainty, such as the impact on agriculture. In the northern regions with fewer heat resources, warming may have a positive impact on plant varieties and planting areas, whereas, in the southern regions with rich heat resources, it may have a negative impact, with food crop yields falling by 24–37% by the second half of the 21st century. The increase in the number of excessive heat resources may also lead to a contradiction between the supply and demand of water resources, resulting in frequent disasters such as droughts and floods, threatening the country's food security. Therefore, analyzing the characteristics of climate change in Northeast China is of great significance for improving the ability to cope with risks, ensuring food stability, promoting economic development, and maintaining social stability. Existing studies have paid more attention to the historical climate change in Northeast China, and there are only a few studies on the future spatiotemporal variations of each meteorological element. The changes in meteorological elements are the basis of research in various fields. In this research, we use a driven regional climate model of the RCP scenarios released by IPCC AR6 to predict future meteorological data and sort out various characteristics of annual average temperature, annual precipitation, and surface net radiation in Northeast China from 2021 to 2099, and further determine the law of climate change. This research is aimed at deepening the comprehensive understanding of high-latitude climate change, and providing the scientific basis for ecological security, water resources security, and food security, thereby ultimately contributing to the international community's joint response to climate change and global sustainable development.

2. Data Sources and Research Methods

2.1 Data sources

The future meteorological data in this study are based on the two emission scenarios of RCP4.5 and RCP8.5, and released by the IPCC 5th Assessment Report. The BCC_CSM regional climate model is used to simulate daily weather data, such as the daily average temperature, daily precipitation, daily net shortwave radiation, and daily net longwave radiation, with a spatial resolution of 0.5 × 0.5° from 2021 to 2099. BCC−CSM1.0 is a multisphere climate system model developed by the National Climate Center, China, and includes atmospheric, land surface, ocean, and sea ice components; each component model is generated by coupled through the coupler CPL5. The atmospheric model BCC_AGCM2.2 has 26 vertical levels and a longitudinal resolution of T16. The longitudinal resolution of the land surface model BCC_AVIM1.0 is T16. The ocean model MOM_L40 has 40 vertical levels and horizontal tripolar grids. The longitudinal resolution is approximately 0.33–1° and the sea ice component is generated by the Sea Ice Simulator (SIS). The model can well reproduce current and future climate changes, especially for the Asian monsoon climate. To facilitate the description of the spatiotemporal changes of meteorological elements, in this study, we separately describe the annual average temperature, annual precipitation, and daily average net surface radiation.(18) To make the simulated value close to the observed value, the original grid data is spatially interpolated in accordance with to the location of meteorological observation stations in Northeast China. The number of meteorological observation stations is 91, and the interpolation method is the bilinear spatial difference. The bilinear spatial difference method is widely used for estimating values at unsampled points within a grid by linearly interpolating in two dimensions. It is computationally efficient and straightforward, making it ideal for large meteorological datasets with relatively smooth spatial gradients. Compared with kriging interpolation, the bilinear spatial difference is less computationally intensive and does not require assumptions about the spatial correlation structure of the data, making it more practical for large-scale applications or datasets with limited spatial continuity information.

2.2 Research methods

In this study, we intend to analyze and discuss the law of time and space changes in temperature, precipitation, and net radiation in RCP4.5 and RCP8.5 to ultimately understand the impact of different policies on climate change. Trend analysis, abrupt change test, and periodic analysis will be used on each meteorological element to discuss the law of time change, and wavelet analysis will be used to discuss the law of spatial change.(19)

2.2.1 Abrupt change test

The moving T test (MTT) was used to test the abrupt changes in the time series of meteorological elements in Northeast China. Since the MTT is an artificially set sliding step, the point of abrupt change may drift. Therefore, in this study, we used the Yamamoto test (YAMA) to test the year with abrupt change. Once again, if two results are consistent, the abrupt year can be basically determined. The specific method is as follows.

MTT is conducted by calculating the following:

$$t = \frac{\bar{x}_1 - \bar{x}_2}{s \cdot \sqrt{\frac{1}{n_1} + \frac{1}{n_2}}} \qquad s = \sqrt{\frac{n_1 s_1^2 + n_2 s_2^2}{n_1 + n_2 - 2}} . \tag{1}$$

YAMA uses the signal-to-noise ratio (*SNR*) to test for significant differences in mean values of different time series:

$$R_{SN} = \frac{\left|\bar{x}_1 - \bar{x}_2\right|}{s_1 + s_2} , \tag{2}$$

where $\bar{x}_1$ and $\bar{x}_2$ are the means of variances of the time series n_1 and n_2, and S_1 and S_2 are the variances of the time series n_1 and n_2, respectively. Generally, $n = n_1 = n_2$ is adopted for continuous variables. In this study, $n = 20$ and $R_{SN} > 0.60$ exceeded the significance level of $\alpha = 0.01$, which was determined as the abrupt point.[20]

2.2.2 Periodic analysis

Wavelet analysis decomposes the time series into the time–frequency domain by wavelet transform to obtain the significant fluctuation pattern of the time series, namely, the periodic change dynamic.

2.2.3 Spatial analysis

The empirical orthogonal function, which can reduce the degree of freedom or dimensionality of data, is used to fully analyze and explore the main and other characteristics of changes in meteorological elements. It has been widely used in disciplines such as meteorology and geography (see Ref. 21 for specific methods). The annual average temperature, precipitation, and average daily radiation in Northeast China are expressed in the matrix $X_{m \times n}$. After standardized processing, a new matrix $N_{m \times n}$ is obtained, where m is the year and N is the number of stations. The specific decomposition is as follows:

$$N_{m \times n} = V_{m \times p} T_{p \times n} , \tag{3}$$

where V is the space eigenvector and T is the time coefficient. When $p = n$ is taken, all meteorological information can be fully described. The main variation characteristics of meteorological elements can be roughly described by feature vectors.[22]

3. Results and Analysis

3.1 Climosequence trend analysis

The mean annual temperature in both scenarios shows a trend of significant increase (Fig. 1). The average temperature in RCP8.5 increases faster by 0.34 °C/10a than that in RCP4.5. From 2021 to 2099, the temperature in the RCP8.5 scenario is about 1.10 °C higher than that in RCP4.5. The precipitation has an increasing trend, being greater in RCP4.5, but the difference between the two scenarios is not significant. The annual precipitation in the RCP4.5 scenario is about 2.19 mm higher than that in RCP8.5. In the future, radiation will show an increasing trend. The radiation in the RCP8.5 scenario will increase faster, and the annual average daily radiation will be 0.12 MJ/(m^2·d) higher than that in RCP4.5.

3.2 Abrupt change monitoring of climosequence

In the RCP4.5 scenario, the year of the abrupt change in average annual temperature is about 20 years earlier than that in the RCP8.5 scenario (Table 1). The abrupt change in the RCP4.5

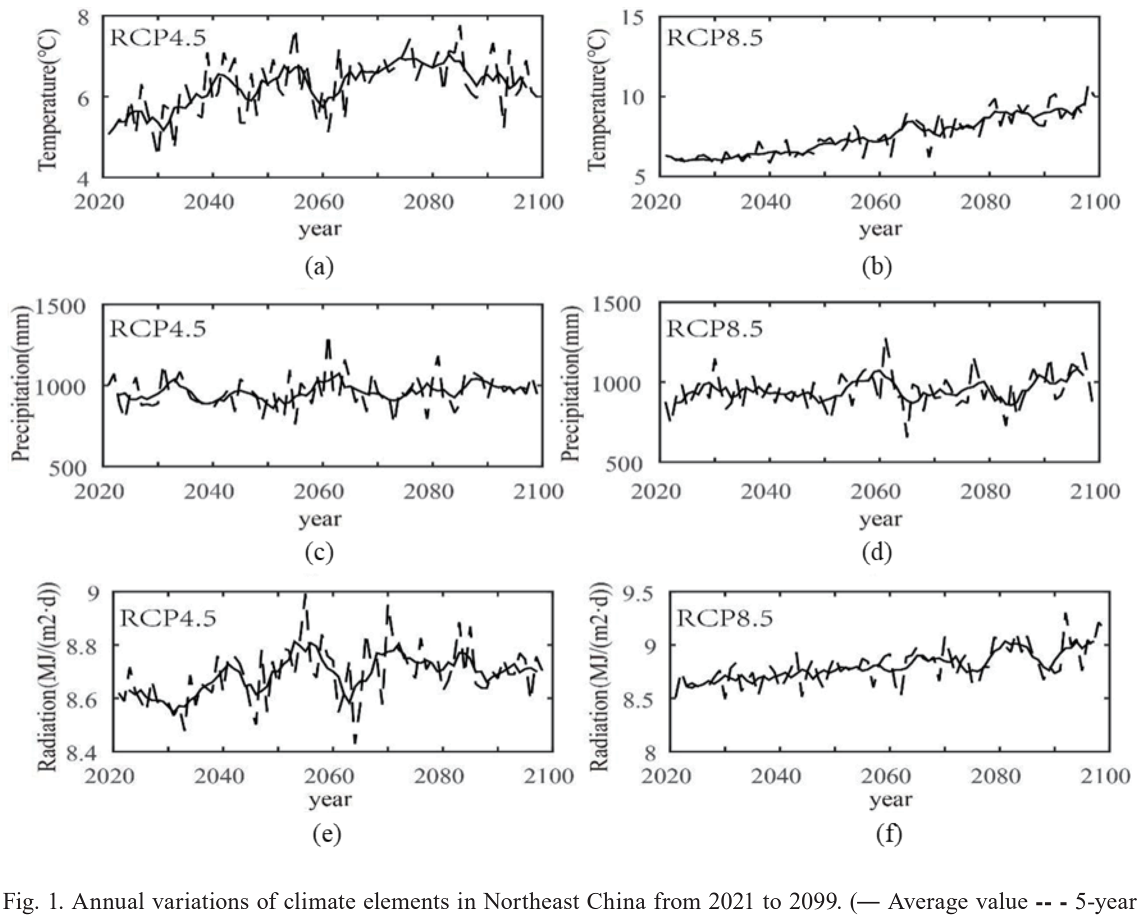

Fig. 1. Annual variations of climate elements in Northeast China from 2021 to 2099. (— Average value -- - 5-year moving average)

Table 1
Abrupt change years of climate elements in Northeast China from 2021 to 2099.

Meteorological Element	Methods	Results											
Scenario		RCP4.5						RCP8.5					
Temperature	MTT	2035	2049*	2058*			2087*	2064		2069*		2080	2090*
	YAMA	2035*	2049		2059	2065*	2087		2065		2071*	2080*	
Precipitation	MTT	2037*	2047*	2057*		2069*		2043*	2054*	2073*		2080*	2088*
	YAMA	2037	2047*	2057	2064			2043	2054*		2075*		2088*
Radiation	MTT	2036	2051	2062	2071	2087*		2064	2073*	2080	2088*		
	YAMA	2036*	2051*	2062	2071*			2064*	2073	2080*	2088		

Note: *indicates that the abrupt change year passed the significance test.

scenario is more concentrated before the 2060s, whereas that in the RCP8.5 is concentrated after the 1960s. The reason for this result may be that people's energy-saving and emission-reduction behaviors in the low-emission scenario will cause the temperature to stabilize or slow down its increase, whereas, in the uncontrolled high-emission scenario, the temperature will continue to rise. Compared with RCP8.5, the abrupt change in average annual precipitation in the RCP4.5 scenario starts earlier and ends earlier. The abrupt annual radiation change in RCP4.5 starts much earlier, and the abrupt time change is more concentrated before the 1960s. The abrupt time change in RCP8.5 occurs after 2064. The MTT and YAMA show the same year of abrupt time change.

3.3 Spatial analysis of climosequence

In the RCP4.5 and RCP8.5 scenarios, the first feature vector field of the annual mean temperature in Northeast China has the same sign (positive) in the whole region (Fig. 2). This shows that the annual mean temperature variation has good spatial consistency and basically represents the main distribution characteristics of the annual mean temperature in Northeast China. This characteristic of regional consistency accounts for 90.26 and 96.61% of the total explained variance in the RCP4.5 and RCP8.5 scenarios, respectively. The maximum absolute value regions are different in both climate scenarios. The maximum absolute value region is around Ulanhot–Tongliao in the west in the RCP4.5 scenario, whereas it is in the northern region in the RCP8.5 scenario. The time coefficient (Fig. 3) corresponding to the feature vector represents the time variation characteristic of the spatial distribution represented by the feature vector in this region. The time coefficient of the first feature vector shows an increasing trend in both scenarios, with that in RCP8.5 increasing faster. The temperature rises faster in the west in the RCP4.5 scenario and faster in the north in the RCP8.5 scenario.

For annual precipitation, in the RCP4.5 scenario, the cumulative explained variance contribution rate of the first three feature vectors is 65.66%, and those of the first, second, and third feature vectors are 45.36, 10.89, and 9.40%, respectively. The first feature vector is a typical field that can indicate the annual precipitation change, which can roughly indicate the spatial variation characteristics of precipitation in the study area. There are positive and negative values

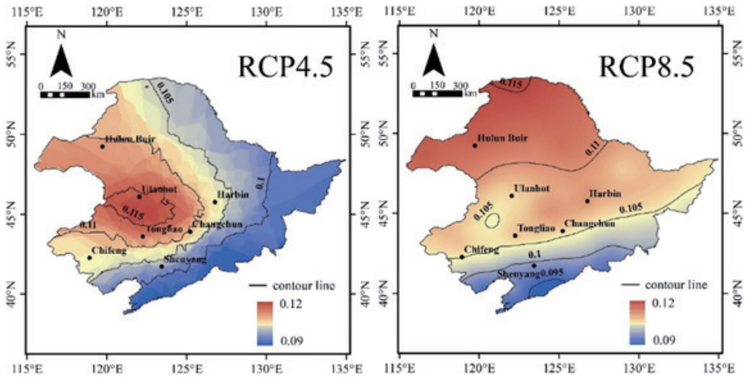

(a) (b)

Fig. 2. (Color online) First feature vector field of annual mean temperature.

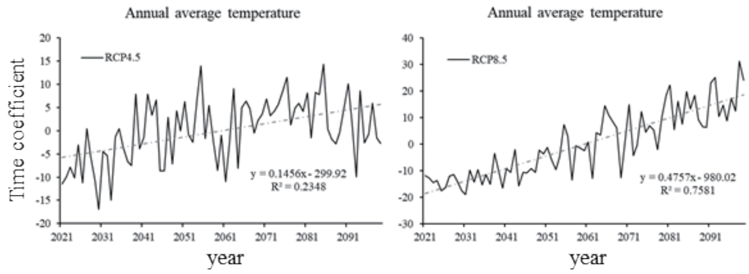

(a) (b)

Fig. 3. First feature vector time coefficient of annual mean temperature.

in the whole region (Fig. 4), with the highest positive value in the southeast and the lowest negative value in the north. This shows that the variation trend of annual precipitation in the two regions is inconsistent. The time coefficient (Fig. 5) shows an overall increasing trend, indicating that precipitation will increase in the southeast and decrease in the north in the future. The change type of the second and third feature vectors is similar to that of the first feature vectors, both with positive and negative values. The time coefficients of the second feature vector are high in the east and low in the west, and those of the third feature vector are high in the north and low in the south. The time coefficients show an increasing trend, indicating that the time coefficient of the second feature vector of precipitation increases in the east and decreases in the west. The time coefficient of the third feature vector increases in the north and decreases in the south.

The explained variance of the first three feature vectors is 66.77% in RCP8.5. The explained variances of the first, second, and third feature vectors are 48.90, 9.19, and 8.67%, respectively. The explained variances of the first feature vectors are all positive in the region, indicating that the annual precipitation change has a spatial consistency and can represent the main characteristics of precipitation distribution. The absolute value in the south is the largest, indicating that the annual precipitation change is the largest in this region. When the time coefficient shows an increasing trend, precipitation will increase in Northeast China and more in

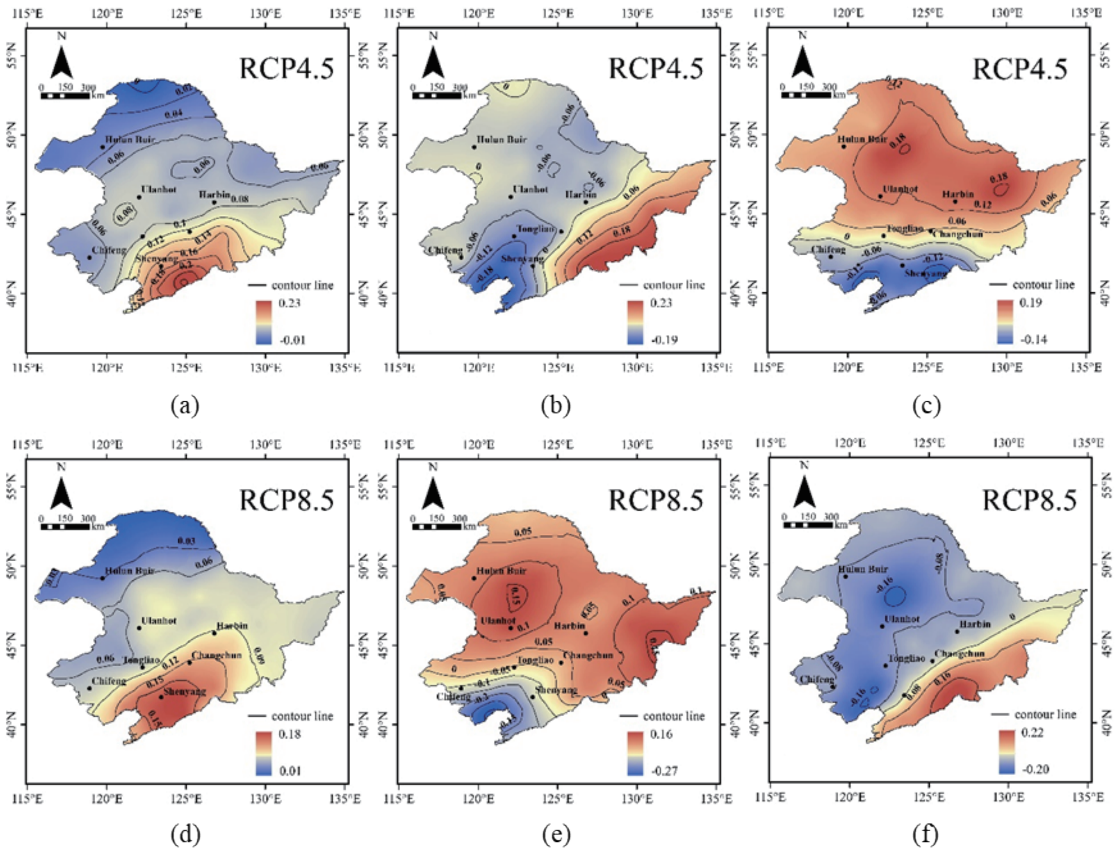

Fig. 4. (Color online) Feature vector fields of annual precipitation. (a, b, and c are the first, second, and third feature vector fields in RCP4.5, and d, e, and f are the first, second, and third feature vector fields in RCP8.5, respectively; the same below)

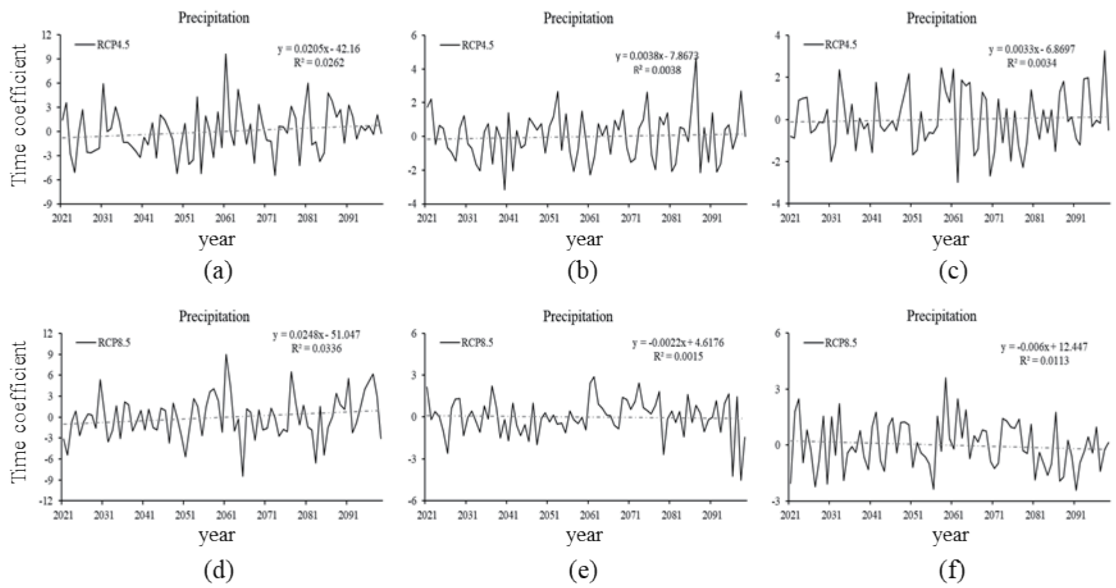

Fig. 5. Feature vector time coefficient of annual precipitation.

the south in the future. The explained variances of the second and third feature vectors are both positive and negative. The explained variances of the second feature vector are high in the north and low in the south, and line 0 is bounded by Tongliao. The explained variances of the third feature vector are high in the southeast and low in the northwest. Line 0 extends from Shenyang-Changchun to the northeast. When the second feature vector time coefficient shows an increasing trend, the precipitation will increase in the north and decrease in the south. When the third feature vector time coefficient shows a decreasing trend, the precipitation will increase in the northwest and decrease in the southeast.

The radiation explained variance of the first three feature vectors is 66.47% in the RCP4.5 scenario. The explained variances of the first, second, and third feature vectors are 42.82, 16.78, and 6.86%, respectively. The explained variance of the first feature vector is positive, indicating that the radiation changes show consistency in space. The eastern region with the highest value is the most sensitive (Fig. 6). The time coefficient shows an increasing trend, and the radiation will increase the most in the eastern region in the future. Both positive and negative values of the second and third feature vectors show that radiation has opposite variation characteristics in different regions under the same general trend. The time coefficient (Fig. 7) of the second feature vector shows an increasing trend, so it can be considered that radiation increases in the

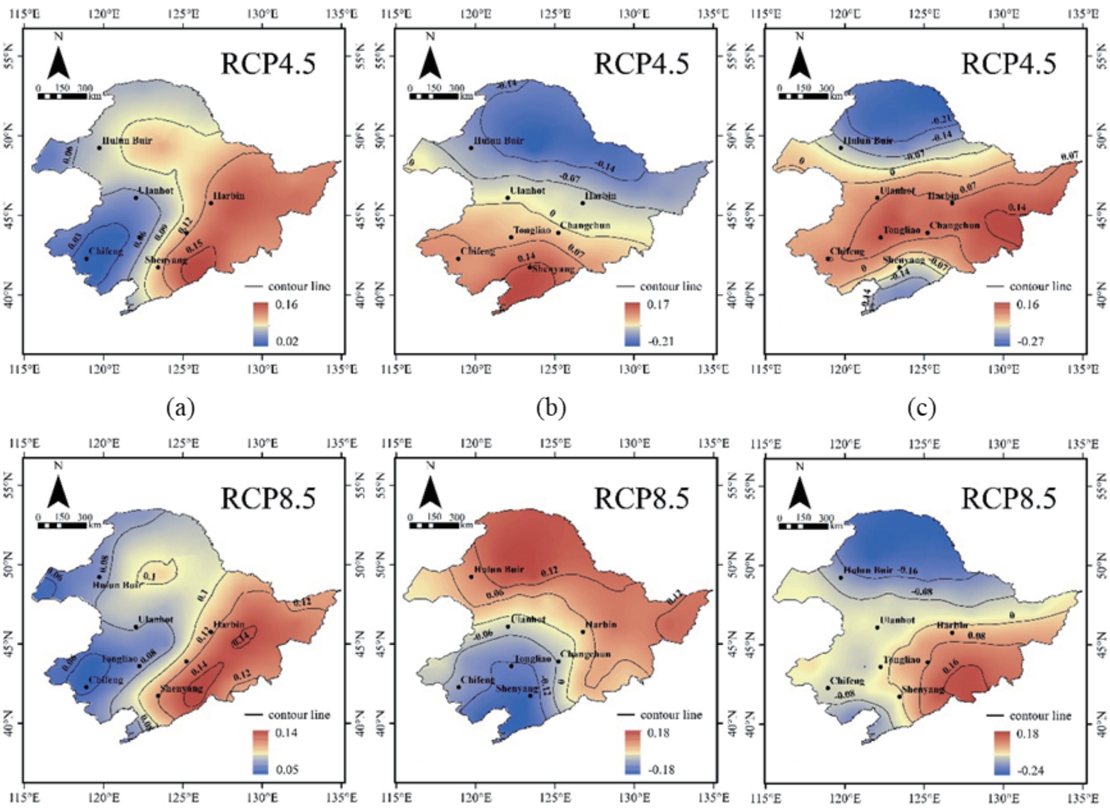

(a) (b) (c)

(d) (e) (f)

Fig. 6. (Color online) Feature vector fields of daily average radiation.

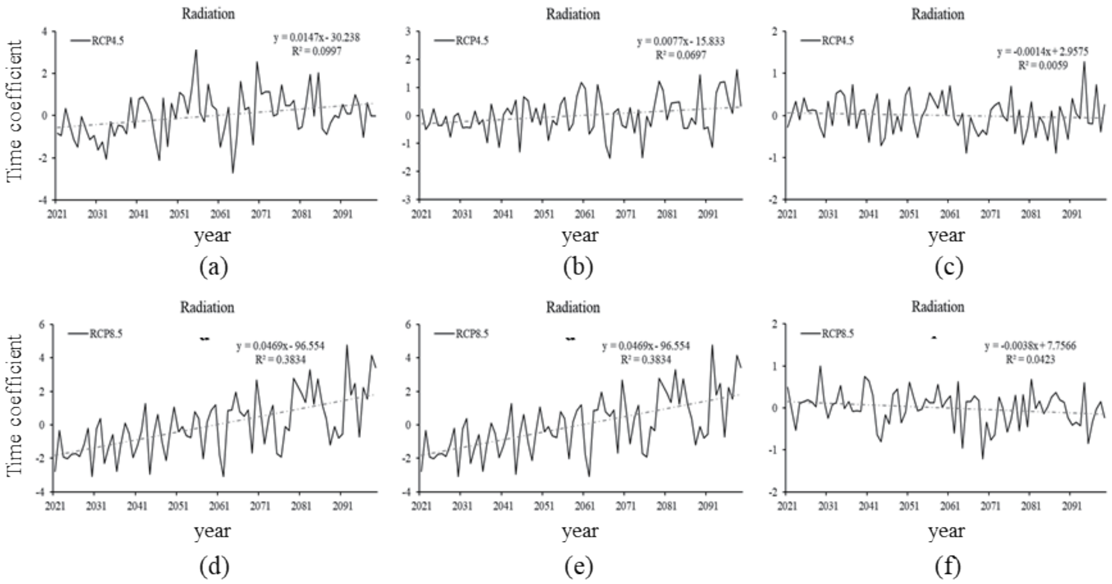

Fig. 7. Feature vector time coefficient of average daily radiation.

south and decreases in the north. When the third feature vector is decreasing, the future radiation will decrease in the central part and increase in the south and north.

The radiation explained variance of the first three feature vectors is 81.38% in the RCP8.5 scenario. The explained variances of the first, second, and third feature vectors are 69.03, 8.31, and 4.23%, respectively. The results of the first feature vectors show that the radiation space variation is consistent and the high-value region is the eastern region. The time coefficient shows an increasing trend, indicating that the radiation will increase the most in the eastern region in the future. The second and third feature vectors have positive and negative values, and the time coefficients show a decreasing trend. The second feature vector of radiation will decrease in the north and increase in the south. The third feature vector will decrease in the southeast and increase in the north.

4. Conclusions

In this study, we used the data simulated in an RCP scenario with high reliability. The scenario is based on the intensity of atmospheric radiation considering the emission policy factor, which makes the research results closer to the real situation and the law of climate change can more accurately analyzed. In previous studies, the climate changes in the traditional Northeastern region were analyzed. For example, with the multimodel data, the temperatures in RCP4.5 and RCP8.5 show an increasing trend from 2016 to 2099, which is consistent with the results of this study. The temperature increase rates in RCP4.5 and RCP8.5 are 0.22 and 0.53 °C/10a, which are 0.07 and 0.04 °C/10a higher than the results of this study, respectively. The precipitation in both scenarios increases and the increase is faster in RCP8.5, but with different rates compared with those in Ref. 23. The factors leading to the above differences may be the differences in time, the area of the study, or the climate model adopted. In this study, only three meteorological elements of radiation, temperature, and precipitation are considered to analyze the law of future climate change. However, in actual production and life, other meteorological elements, such as air humidity and wind speed, will also have a non-negligible impact on people. If the changes in the above-mentioned factors can be considered, the assessment of the law of climate change in Northeast China will be more accurate.

Acknowledgments

This research was funded by the National Key Research and Development Program of China (No. 2022YFD2300201); the Natural Science Foundation of Heilongjiang Province (LH2024D022); the China Postdoctoral Science Foundation Funded Project (Grant No. 2021MD703823); and the Research Fund for the Doctoral Program of Harbin Normal University (Grant No. XKB202202).

References

1 D. Jiang and X. Wang: Trans. Atmos. Sci. **10** (2021) 240. https://doi.org/10.13878/j.cnki.dqkxxb.20210810007
2 B. Su, X. Gao, and C. Xiao: Adv. Clim. Change Res. **15** (2019) 395. https://doi.org/10.12006/j.issn.1673-1719.2019.139
3 Y. Sun: Trans. Atmos. Sci. **8** (2021) 1. https://doi.org/10.13878/j.cnki.dqkxxb.20210816009
4 K. Jiang: Adv. Clim. Change Res. **16** (2020) 251. https://doi.org/10.12006/j.issn.1673-1719.2019.236
5 K. Zhu: Sci. Sin. **02** (1973) 168. http://www.cnki.net
6 J. Yan, Q. Ge, H. Liu, J. Zheng, and H. Fu: Atmos. Clim. Sci. (2014) 211. https://doi.org/10.4236/acs.2014.42024
7 Y. Zhang, X. Shao, Z. Yin, and Y. Wang: Clim. Past. **10** (2014) 1763. https://doi.org/10.5194/cp-10-1763-2014
8 G. Chu, Q. Sun, X. Wang, M. Liu, Y. Lin, and M. Xie: Holocene **22** (2012) 785. https://doi.org/10.1177/0959683611430413
9 Y. Zhao, P. Xiao, and H. Bai: Meteorol. Sci. Technol. **47** (2019) 608. https://doi.org/10.1951/j.1671-6345.20180431
10 R. Huang, L. Xu, and J. Liu: Acta Ecologica Sinica **33** (2013) 4078. https://doi.org/10.5846/stxb201301050030
11 T. Zhou, Z. Chen, X. Chen, M. Zuo, J. Jiang, and S. Hu: Adv. Clim. Change Res. **17** (2021) 1. https://doi.org/0.12006/j.issn.1673-1719.2021.239
12 R. S. Kiani, S. Ali, M. Ashfaq, F. Khan, S, Muhammad, M. S. Reboita, and A. Farooqi: Sci. Total Environ. **788** (2021) 147759. https://doi.org/10.1016/j.scitotenv.2021.147759
13 F. Wang, C. Wang, D. Wu, S. Yao, Y. Bai, and J. Zhang: Chin. J. Agrometeorol. **39** (2018) 398. https://doi.org/10.3969/j.issn.1000-6362.2018.06.005
14 J. Jia and J. Guo: J. Arid Land Reso Environ. **25** (2011) 109. https://doi.org/10.13448/j.cnki.jalre.2011.10.029
15 Y. Liu, F. Yuan, A. Wang, J. Wu, X. Zheng, H. Yin, and D. Guan: J. Appl. Ecol. **30** (2019) 1503. https://doi.org/10.13287/j.1001-9332.201905.006
16 M. Yan, M. Xue, L. Zhang, X. Tian, B. Chen, and Y. Dong: Plants **10** (2021) 821. https://doi.org/10.3390/PLANTS10050821
17 M. Zhou: Study on main climatic factors, mechanism and prediction of grain yield in Northeast China (University of Chinese Academy of Science, Beijing, 2015).
18 Y. Xu: Meteorol. Environ. Sci. **041** (2018) 18. https://doi.org/10.16765/j.cnki.1673-7148.2018.02.003
19 M. Li, J. Xia, S. Chen, and D. Meng: J. Nat. Reso. **06** (2011) 1001. https://doi.org/10.3724/SP.J.1146.2006.01085
20 H. Zhao, L. Gong, H. Qu, H. Zhu, X. Li, and F. Zhao: J. Geogr. Sci. **05** (2016) 585. https://doi.org/10.1007/s11442-016-1287-y
21 B. Tian, M. Yu, and H. Li: Jiangsu Agric. Sci. **46** (2018) 293. https://doi.org/10.15889/j.issn.1002-1302.2018.18.070
22 R. Huang, L. Xu, and J. Liu: Acta Ecologica Sin. **33** (2013) 4078. https://doi.org/10.5846/stxb201301050030
23 C. Tao, C. Jiang, and J. Sun: Acta Geophys. Sin. **59** (2016) 3850. https://doi.org/10.6038/cjg20161006